Zainab Temitope Yaqub[1]
Bilainu Obozokhai Oboirien[1,*]
Marcus Hedberg[2]
Henrik Leion[2]

Experimental Evaluation Using Plastic Waste, Paper Waste, and Coal as Fuel in a Chemical Looping Combustion Batch Reactor

A comparative study of chemical looping combustion (CLC) with paper, plastic, and coal as fuel was carried out. Experiments were performed in a laboratory fluidized-bed reactor by alternating between reduction and oxidation cycles. The results obtained indicated that a higher temperature leads to an increase in the CO_2 yield and carbon conversion for all fuels. Paper had the highest fractional conversion of CO to CO_2 followed by polyvinyl chloride (PVC) and coal. This was due to the higher fraction of volatiles in paper compared to PVC and coal. Scanning electron microscopy (SEM) analysis of the oxygen carrier particle after each of the solid fuel experiment was carried out. For the used ilmenite, there was a slight difference in the morphology for the three different fuels.

Keywords: Chemical looping combustion, Ilmenite, Municipal solid waste, Oxygen carrier, Polyvinyl chloride

Received: October 17, 2020; *revised:* January 21, 2021; *accepted:* March 12, 2021

DOI: 10.1002/ceat.202000501

Supporting Information available online

1 Introduction

The annual emission rate of CO_2 worldwide needs to decrease by 60–80 % to achieve global warming target levels of less than 1.5 °C [1]. Different strategies exist in reducing CO_2 emission into the atmosphere, which include reducing energy consumption, increasing the use of renewable energy sources, and enhancing the biological absorption capacity of forest and soils. However, these efforts are not predicted to be sufficient to attain the CO_2 emission decrease required to meet the maximum 1.5 °C targets. Carbon capture and storage (CCS) has been identified as a strategy for CO_2 emission reduction that can be used to attain a negative net CO_2 emissions environment [2]. There exist different CCS technologies which are employed to reduce CO_2 emissions. Nonetheless, most of the carbon capture technologies have a high energy cost which lessens the energy efficiency of the process, while increasing the cost of energy production [3].

Chemical looping combustion (CLC), on the other hand, is a type of CO_2 separation technology for combustion that has a low energy consumption due to a non-direct contact between fuel and air [4]. This CO_2 capture technology has the ability to combust fuel for efficient heating and electricity generation purposes [5]. CLC has the potential to reduce nitrogen oxide (NO*x*) and dioxin emission when municipal solid waste (MSW) is taken as fuel [6, 7]. The increase in the amount of MSW generated is connected with an increase in population and urbanization and, if not properly managed, it could pose a serious threat to the environment and health of humans [8, 9].

In CLC, the combustion system consists of an air reactor and a fuel reactor. A metal oxide which is referred to as the oxygen carrier (M_xO_y) is introduced into the fuel reactor and as it is reduced, it provides the oxygen needed for the combustion of the fuel [10]. The reduced metal oxide is transferred to the air reactor where it reacts with air and is thus re-oxidized before being reintroduced into the fuel reactor, hence forming a loop. Since fuel and air do not mix in the same reactor, there is no additional cost for CO_2 separation in this method [11].

Fig. 1 presents the description of a CLC process as depicted by Adanez et al. [12]. An oxygen carrier suitable for CLC must be highly reactive to air and fuel [13]. The oxygen carrier must have the ability to undergo repeated oxidation-reduction cycles, and should be environmentally friendly and cheap [14]. Some solid fuels contain large amounts of ash which can deactivate the oxygen carrier. Due to this reason, it is beneficial to use an oxygen carrier that is inexpensive and can be easily replaced. Therefore ores, such as ilmenite, are often used as oxygen carriers for solid fuels [15, 16].

[1]Zainab Temitope Yaqub, Prof. Bilainu Obozokhai Oboirien
boborien@uj.ac.za
University of Johannesburg, Department of Chemical Engineering Technology, Doornfontein, 2028, South Africa.

[2]Dr. Marcus Hedberg, Prof. Henrik Leion
Chalmers University of Technology, Department of Chemical and Biological Engineering, 412 96 Göteborg, Sweden.

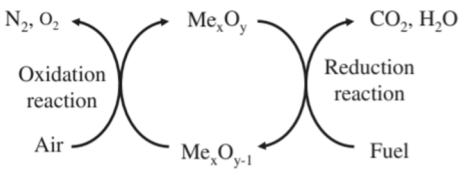

Figure 1. Layout of a CLC process [6].

CLC for solid fuels can be categorized depending on whether the solid fuel directly or indirectly reacts with the oxygen carrier. The first approach is to carry out solid gasification in a gasifier, and the syngas produced is then introduced into the CLC system [17, 18]. The second approach is when the solid fuel is introduced directly to the CLC fuel reactor (solid-fueled CLC). The solid-fueled CLC is further classified into in-situ gasification CLC (IG-CLC) and chemical looping oxygen uncoupled (CLOU) [19]. Most experiments are operated under a fluidized-bed condition using the IG-CLC process because it does not require a gasifier and favors the solid-gas interaction [20].

When the solid fuel is fed into the fuel reactor, devolatilization takes place and volatiles and char are generated. The char undergoes gasification with steam and/or CO_2. The volatiles and gasification products react with oxygen carriers to produce the combustion products according to Eqs. (1)–(4).

$$\text{Solid fuel} \rightarrow \text{volatile matter} + \text{char} \quad (1)$$

$$\text{Char(C)} + CO_2 \rightarrow 2CO \quad (2)$$

$$\text{Char(C)} + H_2O \rightarrow CO + H_2 \quad (3)$$

$$M_xO_y + \text{volatile} + CO + H_2 \rightarrow M_xO_{y-1} + CO_2 + H_2O \quad (4)$$

The steam is condensed and pure CO_2 is obtained. The reduced oxygen carrier gets re-oxidized in the air reactor as seen in Eq. (5):

$$M_xO_{y-1} + \frac{1}{2}O_2 \rightarrow M_xO_y \quad (5)$$

One of the challenges faced with the IG-CLC is the incomplete conversion of char in the fuel reactor. When this occurs, the unconverted char moves to the air reactor where CO_2 is produced. This reduces the CO_2 capture efficiency of the process. Several solutions were proposed for limiting the amount of unreacted char that is being transported to the air reactor. The application of a carbon stripper was found to improve the performance of the system by separating the unreacted char from the oxygen carrier before being transported to the air reactor [21, 22]. Also, an oxygen polishing step was proposed by Gayan et al. to complete the combustion process and hence reduce the amount of unreacted char available [23].

Different solid fuels such as coal, wood pellets, biochar, biomass, and even some components of MSW were tested in experimental CLC systems to evaluate combustion efficiency, carbon capture efficiency, and the effects of different oxygen carriers [24, 25]. Studies were performed on different oxygen carriers and their impact on the efficiency in CLC. Low-cost oxygen carriers such as iron ore [15, 26], manganese ore [27, 28], ilmenite [25, 29] ,and industrial waste materials such as bauxite [30] were used for various CLC experiments. A mixture of different oxygen carriers was also studied and improved gas conversion was noticed as a result [31].

Perez-Vega et al. [32] evaluated the effect of manganese-iron mixed oxide doped with titanium as an oxygen carrier in CLOU of coal. The oxygen carrier showed high potential and the combustion efficiency of the solid fuel improved as the oxygen uncoupling capability was enhanced at suitable operating conditions in the air reactor. Bhui and Vairakannu [33] reviewed the chemical looping co-combustion of coal and biomass to reduce carbon emission. The blending of coal and biomass in CLC was noticed to have a higher carbon conversion due to the presence of ash which serves as a catalyst and the high proportion of volatile matter present in the solid fuels.

Fan et al. [34] investigated the performance of a coal gasification CLC combined with cooling, heating, and power production. The thermodynamic evaluation of the process indicated that the overall energy efficiency of the process was between 58–60 %. The CLOU and the IG-CLC processes were also compared based on the reactivity using CuO as an oxygen carrier and coal as solid fuel [35]. A lower carbon conversion rate was noticed in the IG-CLC when compared to the CLOU.

With regard to MSW as solid fuel, few CLC studies were carried out. Bi et al. [36] combusted a type of plastic waste, polyvinyl chloride (PVC) and kitchen waste using Fe_2O_3 as the oxygen carrier. The oxygen carrier was found to absorb the chlorine after the reduction stage and reduce the amount of dioxins emitted [36].

The adsorption property of copper- and iron-based oxygen carriers in cadmium was investigated by Chen et al. [37]. Cadmium, which is present in MSW, can lead to the formation of cadmium oxide during combustion. It was observed that 90 % of the cadmium in the MSW was distributed in the oxygen carrier and can be detached gradually in the chemical looping gasification process [37]. Ma et al. [38] evaluated the performance of iron ore and a CaO adsorbent as an oxygen carrier in IG-CLC of plastic waste. A combustion efficiency of 98 % was achieved, and the results also showed that the addition of the adsorbent helps to reduce the formation of dioxins without altering the properties of the oxygen carrier.

There exist no reports on the CLC of paper, which is a key component of MSW. Also, no study compared the CLC of plastic, paper, and coal in a fluidized-bed CLC. However, Chemcad software was used to predict the performance of CLC of waste paper, plastic components, and paper/plastic blends which was compared with that of South African coal. The result of the simulation indicated a close CO_2 yield between paper, plastic, and coal but a better yield was observed for the blends at all different blend ratios tested [39]. This study evaluates the combustion efficiency of waste paper, plastic waste, and coal in a fluidized-bed reactor using ilmenite as the oxygen carrier at different temperatures.

2 Methodology

2.1 Experimental Setup

The experiment was conducted at the Environmental Inorganic Chemistry Laboratory of the Chalmers University of Technology, in a batch fluidized-bed reactor. The experimental procedure was the same as that described by Keller et al. [40]. A schematic overview of the laboratory setup is depicted in Fig. 2 and by Leion et al. [14].

2.2 Material Preparation

South African ilmenite ore served as oxygen carrier. Ilmenite has been reported to have a high oxygen transport capacity and good fluidization behavior [41]. The ilmenite sample was calcined in air at a temperature of 900 °C at a heating rate of 5 °C min^{-1} for 3 h and cooled at 10 °C min^{-1} to remove any organic impurities present. Calcining the oxygen carrier before experiments also guaranteed that the oxygen carrier was introduced into the reactor in its most oxidized state. This also helps to avoid mass gain during heating up of the oxygen carrier during experiments and thus simplifies the mass balance during calculations. The treated metal oxide was crushed and sieved and a particle size of 125–180 µm was selected in this experiment.

Syngas activation was done to evaluate the reactivity of the oxygen carrier before testing with the solid fuels [42]. In this case, syngas was used as fuel in the reduction cycle with the oxygen carrier. This was done by placing 15 g of the oxygen carrier inside the fluidized-bed reactor and exposing it to 450 mL min^{-1} of syngas for four cycles at a reaction temperature of 950 °C. This is to ensure the stability of the reactivity of the oxygen carrier before being used for the solid fuel. For the solids fuel experiment, a gas flow of 900 mL min^{-1} was chosen for both reducing and oxidizing periods. The experiments were performed at a reactor temperature of 800–950 °C. Steam and nitrogen served as a fluidizing gas and were introduced at the same time as the solid fuel was introduced into the reactor. Nitrogen gas was also added to the top of the reactor to sweep down the solid fuel and to prevent condensation of the steam in the inlet of the solids fuel. However, the sweep gas never reached the reaction zone of the reactor. The flue gas from the cooler gets transferred to the gas analyzer (Rosemount NGA-2000) and the concentrations of CO, CO_2, CH_4, and O_2 were measured and recorded.

The oxidation in the fluidized bed was done at 5 % O_2 in nitrogen. The re-oxidation of the oxygen carrier for each cycle was carried out until the outlet oxygen concentration was stable and the initial oxygen concentration was 5 % in volume. After each oxidizing and reducing period, nitrogen gas was introduced (inert period) to avoid mixing of the gases from oxidizing and reducing phases. Each cycle was performed at least twice to ensure a steady reaction. The reduced form of ilmenite used was $FeTiO_3$ and the most oxidized form Fe_2TiO_5 + TiO_2, which stoichiometrically corresponds to Fe_2O_3 + 2TiO_2 [43], being 5 % of the theoretical oxygen transfer capacity [41]. It should be noted that the oxygen carrier was heated up until 950 °C and cooled to room temperature at the end of each experiment.

South Africa coal, paper, and PVC samples were selected as solid fuels. The particle size of the solid fuels ranged from 125–180 µm. The properties of the fuels used are stated in Tab. 1. For each reduction cycle 0.1 g of the solid fuel sample was taken. Each experimental cycle was repeated at least twice and the average value was used to analyze the result.

2.3 Data Evaluation

The degree of carbon conversion helped to evaluate the progress of char conversion during reduction. It is defined as the ratio of the mass of carbon already gasified to the total mass of carbon entering into the reactor. This is evaluated by integrating the carbon-containing flue gases during reduction and dividing by the integration of the carbon-containing flue gas during reduction and oxidation as described by Keller et al. [40]. The reduction phase was evaluated to range between 30 %

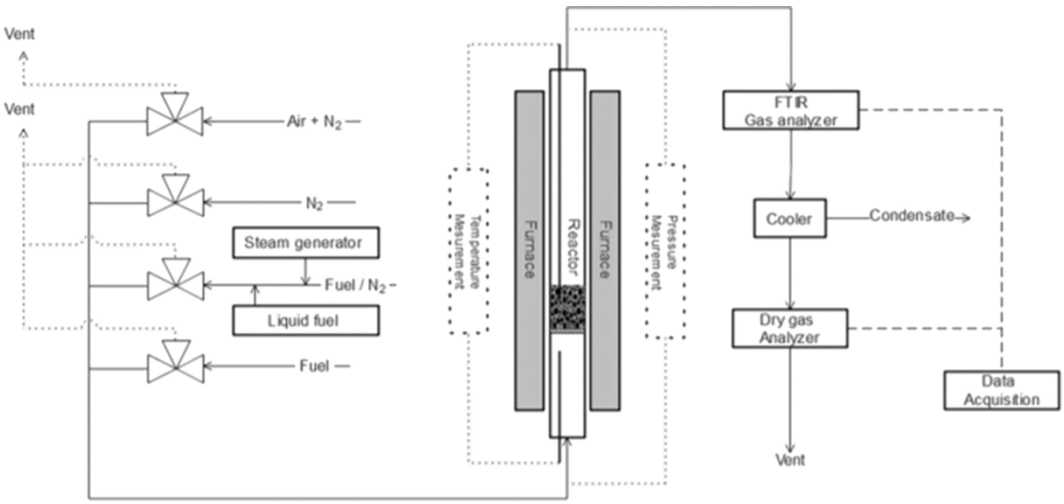

Figure 2. Laboratory setup of the fluidized-bed system used in the experiment [14].

Table 1. Characterization of the three solid fuel samples.

Fuel	Proximate analysis [wt %]			Ultimate analysis [wt %]						Heating value [MJ kg^{-1}]
	Volatile	Moisture	Ash	C	H	N	S	O	Cl	
Waste paper	76	3	12	35.6	4.6	0.6	–	43.3	0.9	12.28
PVC	69	–	14	35.6	4.01	0.5	–	0.5	59.3	15.55
South Africa coal	22.7	2.1	37.5	78.4	4.5	1.8	1.0	14.3	–	19.82

and 70 % carbon conversion by Keller et al. [40]. The gasification period was used to determine the overall performance of the CLC system since it is the limiting reactant step. The degree of carbon conversion can be calculated as Eq. (6):

$$X_c = \frac{m_c(t)}{m_{total}} \tag{6}$$

where $m_c(t)$ is the mass of carbon converted up until time t, and m_{tot} is the total mass of carbon that entered into the reactor from the beginning of the gasification up until the end of the oxidation cycle.

The rate of carbon conversion, r_w, was evaluated by defining carbon conversion as a function of time. This was used to compare the CLC conversion rate of the fuel samples (Eq. (7)).

$$r_w = \frac{dX_c}{dt} \tag{7}$$

The CO fraction was defined as the cumulative amount of carbon converted to CO at a given conversion divided by the total amount of fuel released as CO, CH_4, and CO_2 during an entire cycle. This was used to analyze the effect of temperature on unconverted CO (Eq. (8)).

$$\text{CO fraction} = \frac{CO_{CUM}}{(CO + CO_2 + CH_4)_{total}} \tag{8}$$

3 Results

3.1 CLC of Paper Waste

The outlet concentrations of the measured gases, when paper is used as fuel, as a function of time for the reducing period at 800 °C are displayed in Fig. 3a. The devolatilization occurs immediately when the fuel sample entered the reactor as the paper contains a high fraction of volatiles. The char reaction and the devolatilization occur almost simultaneously and could not be separated, unlike when compared with the slow reacting petroleum coke used by Leion et al. [44] where different peaks were noticed for the devolatilization and char gasification reactions. The gas concentrations start to decrease after an average of 15 s and all the paper samples are completely reacted after 1.5 min. The presence of CO in the gas concentration is due to the insufficient contact between the gasification products and the oxide carrier, hence it could not be fully converted to CO_2.

During the oxidation stage, the oxygen present in the oxidation flow reacts with the reduced oxygen carrier while the

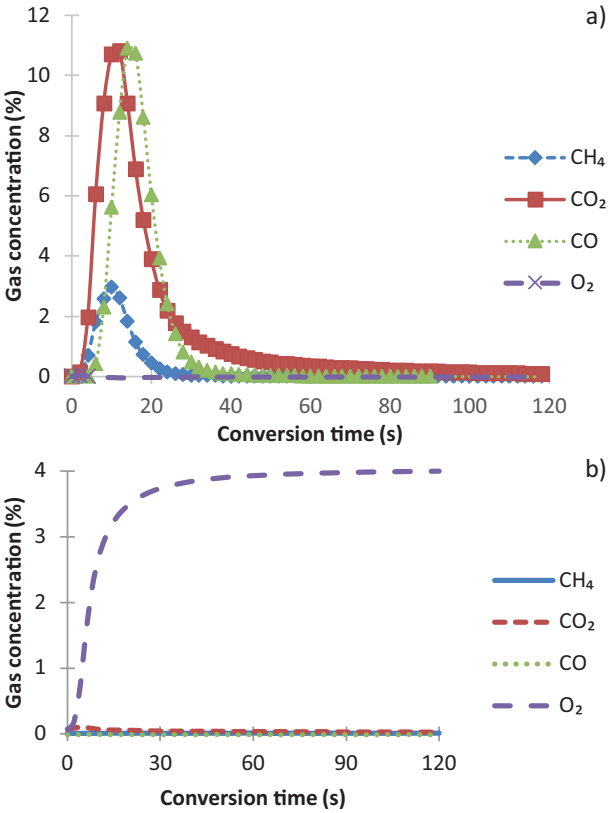

Figure 3. (a) Gas concentration profile during the reduction of CLC of paper waste (800 °C), (b) gas concentration profile during oxidation of ilmenite of CLC of paper waste (800 °C).

nitrogen (N_2) is inert in the reactor. The oxidation of the oxygen carrier takes place at 5 % oxygen concentration. All oxygen is consumed during the first 20 s. The oxygen concentration then increases rapidly until it becomes constant at 5 % as seen in Fig. 3b. It can be observed that little outgoing carbon-containing gases are present during the oxidation. This is because no char exists in the bed and all the carbon present iss consumed during the gasification process. The small amount still detected is assumed to be carbon left in the feeding system and the upper filter of the reactor.

3.2 CLC of Plastic Waste

A similar trend for the gas concentration profile in the reduction phase is noticed when PVC is used as the solid fuel

(Fig. 4), but with lower outlet gas concentration and a longer fuel conversion time compared to paper in Fig. 3a in Sect. 3.1. This is because the volatile content in PVC is lower than that of paper, hence the rate of reaction will be lower. The shape of the gas concentration curves also indicates an initial peak with mainly volatile conversion followed by a tail with slower char conversion. It should also be noted that the concentration of methane in the outlet gas when PVC was used as fuel was higher than that of CO at the beginning of the gasification cycle and reduces drastically towards the end of the cycle as observed in Fig. 4 below. This is because the initial devolatilization step occurs quickly at the initial stage and favors the production of hydrocarbons [7, 45]. It was found that the oxygen concentration trend during oxidation is the same for all the different solid fuels tested as the same parameters were employed.

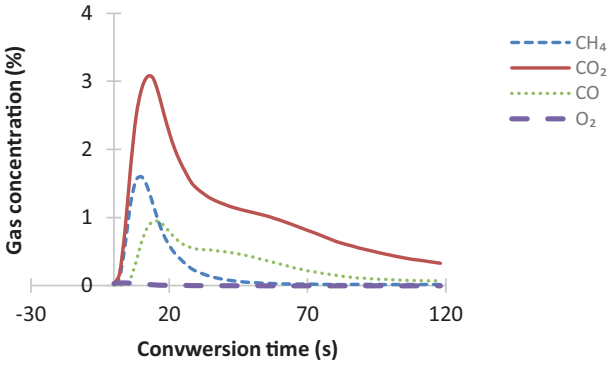

Figure 4. Gas concentration profile during the reduction of CLC of PVC waste (800 °C).

3.3 CLC of Coal

The CLC of South African coal was also performed to evaluate the effect of the reduction time compared to the other fuels. It was noticed that it takes a longer time for the coal to be converted (Fig. 5) compared to paper and plastic. This is because of its low volatile matter in comparison to paper and PVC. The char gasification step in coal is very slow, and some amount of char is still present in the reactor which still reacts after the 120 s presented in the plot.

3.4 Average Rate of Reaction in the CLC of Paper, Plastic, and Coal

The average rate of fuel conversion as a function of fuel converted during the CLC of South African coal, PVC, and paper sample was compared. This was done at 800 °C and is illustrated in Fig. 6. The rate of reaction rises as the conversion increases until it gets to a certain conversion when most of the carbon has been converted and

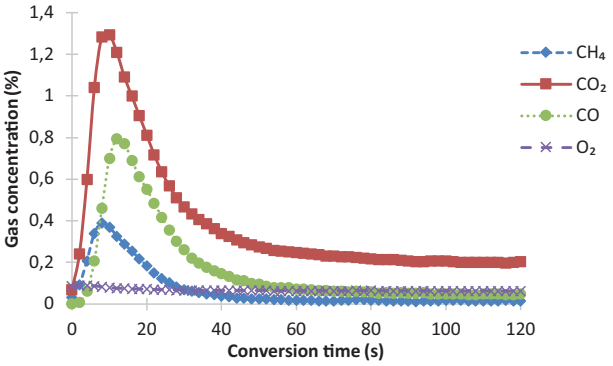

Figure 5. Gas concentration profile during reduction of CLC of coal (800 °C).

the rate decreases. Paper has the highest rate of reaction followed by PVC and lastly coal. It takes less than 30 s for 95 % conversion to be achieved for paper, about 3 min for PVC while that of coal was around 10 min. However, it should be noted that in the case of coal there was still char left in the reactor and the full conversion is then even longer. The reason is the higher volatile content present in the paper as compared to PVC and coal according to Tab. 1. Similar results were reported by Leion et al. [46, 47] for different solid samples in a wide range of volatile content.

3.5 Effect of Temperature on the CLC of Paper, Plastic, and Coal

Fig. 7a demonstrates the trend of the mass of carbon converted to CO and CO_2 during the reduction cycle of CLC of paper at different temperatures. The change in temperature is very little on the mass of the carbon converted to flue gases. This is again due to the very high volatile content since the volatiles leave as

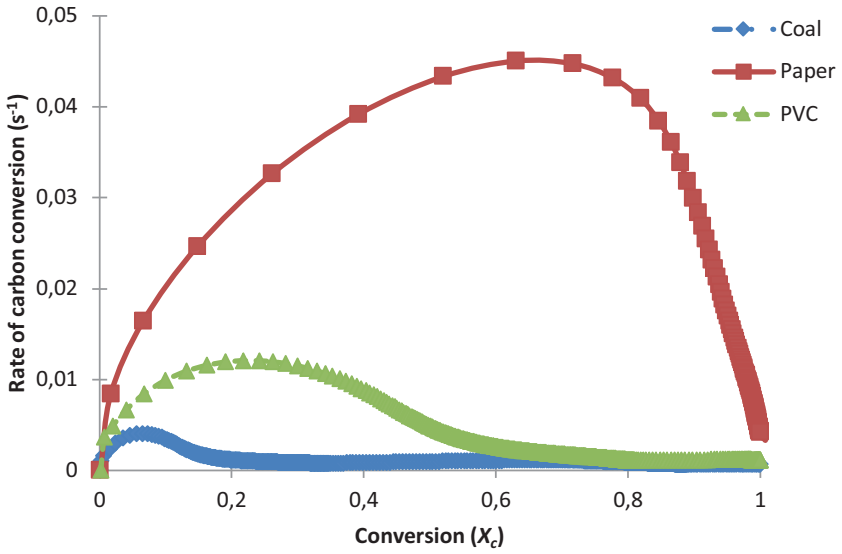

Figure 6. Rate of carbon conversion as a function of the degree of carbon conversion for paper, PVC, and coal.

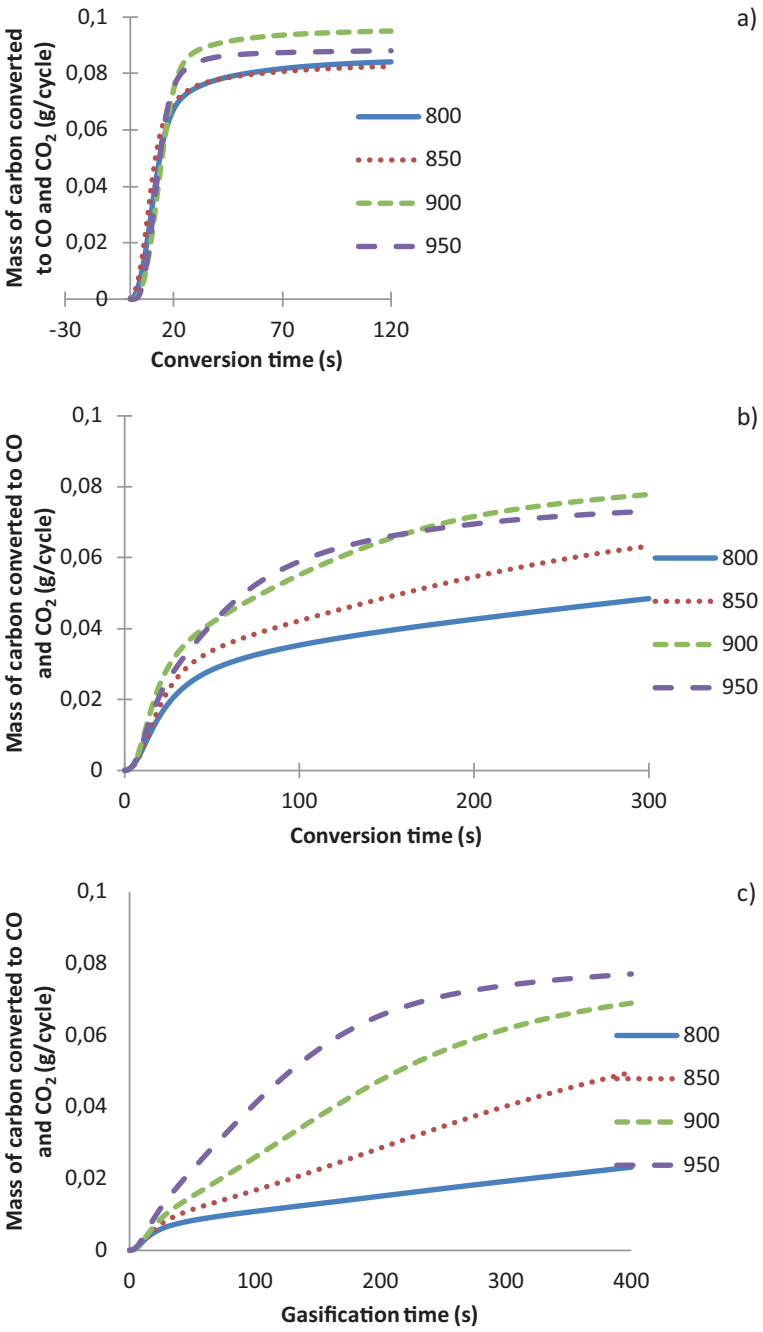

Figure 7. Mass of carbon converted to CO and CO_2 as a function of time during reduction at different temperatures for (a) paper, (b) PVC, and (c) coal.

soon as the fuel enters the reactor even at the lower 800 °C. However, the case is different for PVC and coal as the influence of the increase in temperature was quite noticeable (Figs. 7b and 7c). As the temperature rises, the mass of the carbon-containing gases also increases from 800–950 °C. This is due to higher rates of gasification of the char fraction as the temperature increments [48]. However, the highest concentration of carbon-containing flue gas for PVC seems to be similar at 900 °C and 950 °C as opposed to that of coal (Fig. 7c) below which it was increased up to 950 °C. This could be because of the comparably low fraction of char in the PVC making it hard to see any difference in conversion at these temperatures.

The same trend is also observed when the average rate of reaction of PVC is plotted against its conversion (see Supporting Information). This infers that increasing the temperature for CLC of PVC to 950 °C is not necessary to reach high conversion. Fig. 8 illustrates how the average rate of conversion rises during gasification (30–70 % conversion) at higher temperature for all the fuels tested. It can be inferred that at a higher temperature the rate of conversion is also increased. Thus, at a higher temperature higher carbon capture efficiency and carbon conversion can be achieved as also illustrated in the literature [49]. The effect of CO fraction from the flue gas at different temperatures for the three solid fuels is also analyzed and further explained in the Supporting Information.

3.6 Morphology of Oxygen Carrier Used in CLC of Paper, Plastic, and Coal

Fresh ilmenite after heat treatment and ilmenite obtained after CLC of paper, plastic, and coal experiments were investigated with scanning electron microscopy (SEM). The SEM micrographs are presented in Figs. 9a–d. The used ilmenite has smoother edges and rougher surfaces than the fresh ilmenite. Similar results have been reported before [46]. The changes in the surface edges are due to the high temperature and compression of particles that occurred during the oxidation and reduction reaction and also due to attrition during fluidization [50]. Sintering is observed on the surface of the reacted ilmenite. This could be due to the reactivity deterioration of the oxygen carrier [51], high temperature or as a result of ash from the fuel. However, no ash was detected.

The Brunauer-Emmett-Teller (BET) analysis of the fresh and used ilmenite was performed. The surface area of the fresh ilmenite (1.76 m^2g^{-1}) was found to be higher than that of the used ilmenite for paper (0.44 m^2g^{-1}), PVC (0.73 m^2g^{-1}), and coal (0.26 m^2g^{-1}). The ilmenite particles in CLC of coal has the highest surface roughness followed by PVC and lastly that of paper. The reason for the slight difference in the morphology of the used ilmenite for the three fuels might be related to the degree of reactivity deterioration of the oxygen carrier. This means that used ilmenite of coal has the highest degree of deterioration, followed by that of paper and lastly PVC. However, Khakpoor et al. [52] indicated that the slight change in the surface area of fresh and used ilmenite could be considered insignificant and has little or no effect on the reactivity of the oxygen carrier.

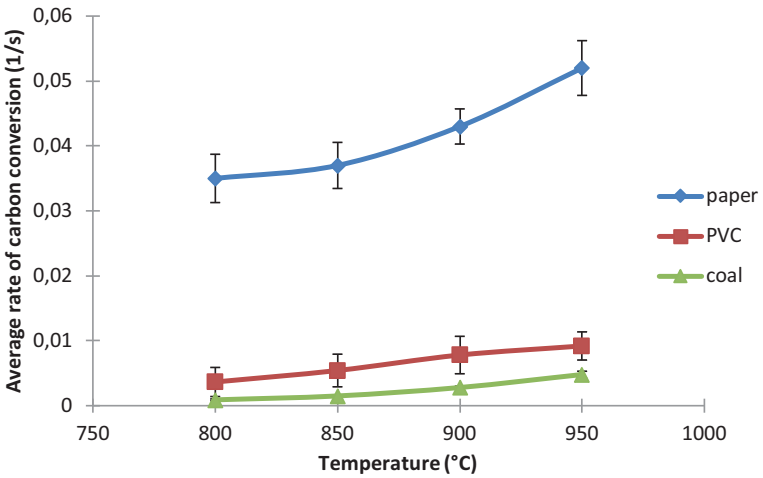

Figure 8. Average rate of conversion from 30–70 % conversion for paper, PVC, and coal at different temperatures. Note: the error bars for the coal experiment are very narrow, hence not seen in the figure.

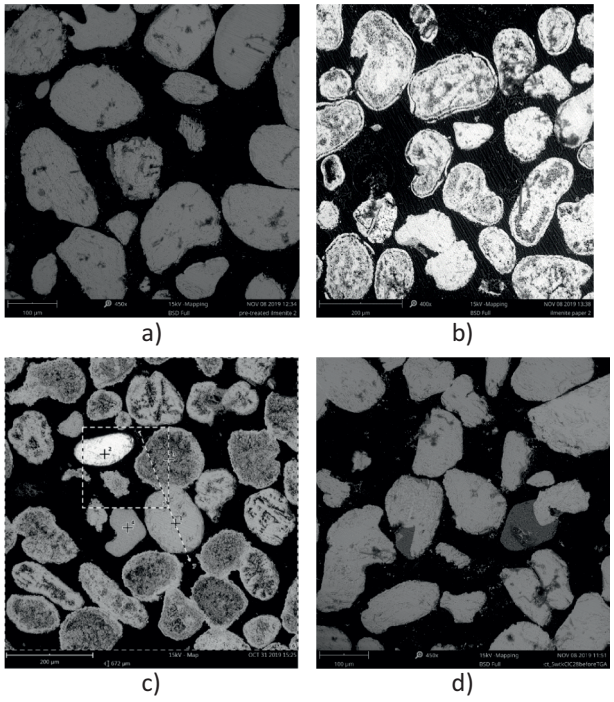

Figure 9. SEM micrograph of (a) fresh ilmenite, (b) ilmenite used in CLC of paper, (c) ilmenite used in CLC of PVC, (d) ilmenite used in CLC of coal.

4 Discussion

This paper describes the CLC of solid waste (paper and PVC) and coal using a batch fluidized-bed reactor. Previous work on CLC of MSW [7, 38] described the effect of different strategies to improve the carbon conversion, combustion efficiency, and suitable oxygen carriers that can help in reducing dioxin emissions, a persistent organic pollutant that is usually emitted during incineration of MSW. This experiment shows the prospect of capturing CO_2 using MSW in a fluidized-bed reactor with ilmenite as an oxygen carrier. The presence of unreacted gases (CO, CH_4) in the CLC of solid fuels can be due to different reasons: the amount of volatiles present in the fuel, the low reactivity of the oxygen carrier, or bad mixing in the reactor with gasification in the upper part of the reactor not giving gasification products enough time to react. This can be reduced by either separating and recycling the unconverted gas or by adding another fuel reactor in series with the first [53]. It is also possible that a different reactor design can improve the conversion where fuel is inserted into the bed and not, as in this case, dropped on top of the bed. Also, different oxygen carriers with higher reactivity to H_2 and CO or an oxygen carrier with CLOU properties would help in increasing the carbon conversion.

Cuadrat et al. [54] also examined the influence of adding limestone ($CaCO_3$) to the reactor bed to increase the gas conversion by experimenting with the CLC of pet coke with ilmenite as an oxygen carrier. The presence of lime would serve as a catalyst in the water-gas shift reaction and improves the CO_2 capture by increasing the char gasification rate [54]. Also, potassium-modified ilmenite was found to improve the CO_2 capture in CLC of coal due to the catalytic effect of potassium on char conversion [55, 56].

The rate of carbon conversion of MSW (paper and PVC) was compared with that of South African coal. The graph in Fig. 6 in shows a faster residence time and a higher rate of carbon conversion in paper and PVC than in coal. This further indicates the operability and the adaption of the fluidized-bed system in the CLC of MSW.

A different trend of carbon mass converted to CO and CO_2 was observed for the solid fuels tested at different temperatures with coal having a higher amount of carbon converted as the temperature increases. This trend is similar to that found in literature irrespective of the oxygen carrier used [57, 58]. As explained in previous works, increasing the temperature enhances the char gasification and also raises the reaction rate between oxygen carriers and volatiles. However, for PVC the smaller amount of carbon converted is likely due to the low amount of char present and the high amount of chlorine in the sample. This might have led to the blow-off of some of the PVC samples during the reduction process which makes it difficult for most of the carbon to be converted.

The CLC experiment carried out on the waste samples (paper and plastic) and coal demonstrates a high CO_2 capture. The high CO_2 concentration produced during CLC makes the process a clean and efficient waste-to-energy technology. The experimental analysis can be used to optimize the design of the CLC unit by scaling up and further development of the technology. However, the challenge with scale-up is reducing the amount of unburnt char present in the combustion chamber. Several measures have been proposed to reduce the presence of unburnt char. This includes the addition of a carbon stripper and improving the gas-oxygen carrier contact by incorporating new designs into the current CLC unit [54].

5 Conclusion

Based on the comparative analysis of CLC of paper, plastic, and coal with ilmenite, the following conclusions can be drawn:

- The average rate of reaction of paper was faster than that of PVC and coal. This was due to the higher volatile content of paper compared to PVC and coal.
- The mass of carbon converted improved when the temperature was increased, which can be attributed to a higher reaction rate as the temperature increases.
- The fractional conversion of CO to CO_2 was highest in paper, followed by PVC and lastly coal.

Acknowledgment

This work was made with the financial support from the University of Johannesburg and Chalmers University of Technology.

The authors have declared no conflict of interest.

Supporting Information

Supporting Information for this article can be found under DOI: https://doi.org/10.1002/ceat.202000501

Abbreviations

BET	Brunauer-Emmett-Teller
CCS	carbon capture and storage
CLC	chemical looping combustion
CLOU	chemical looping oxygen uncoupling
IG-CLC	in situ gasification chemical looping combustion
MSW	municipal solid waste
PVC	polyvinyl chloride
SEM	scanning electron microscopy

Data Availability Statement

Data available on request from the authors

References

[1] V. Masson-Delmotte et al., *Summary for Policymakers. In: Global Warming of 1.5 °C. An IPCC Special Report on the Impacts of Global Warming of 1.5 °C above Pre-Industrial Levels and Related Global Greenhouse Gas Emission Pathways, in the Context of Strengthening the Global Response To*, Switzerland **2018**.

[2] A. Raza, R. Gholami, R. Rezaee, V. Rasouli, M. Rabiei, *Petroleum* **2019**, *5 (4)*, 335–340. DOI: https://doi.org/10.1016/j.petlm.2018.12.007

[3] M. M. Hossain, H. I. de Lasa, *Chem. Eng. Sci.* **2008**, *63 (18)*, 4433–4451. DOI: https://doi.org/10.1016/j.ces.2008.05.028

[4] A. Nandy, C. Loha, S. Gu, P. Sarkar, M. K. Karmakar, P. K. Chatterjee, *Renewable Sustainable Energy Rev.* **2016**, *59*, 597–619. DOI: https://doi.org/10.1016/j.rser.2016.01.003

[5] L. S. Fan, L. Zeng, W. Wang, S. Luo, *Energy Environ. Sci.* **2012**, *5 (6)*, 7254–7280. DOI: https://doi.org/10.1039/c2ee03198a

[6] J. Adanez, A. Abad, F. Garcia-Labiano, P. Gayan, L. F. De Diego, *Prog. Energy Combust. Sci.* **2012**, *38 (2)*, 215–282. DOI: https://doi.org/10.1016/j.pecs.2011.09.001

[7] H. Zhao, J. Wang, *Combust. Flame* **2018**, *191*, 9–18. DOI: https://doi.org/10.1016/j.combustflame.2017.12.026

[8] H. Tian, J. Gao, L. Lu, D. Zhao, K. Cheng, P. Qiu, *Environ. Sci. Technol.* **2012**, *46 (18)*, 10364–10371. DOI: https://doi.org/10.1021/es302343s

[9] O. Eriksson, G. Finnveden, *Energy Environ. Sci.* **2009**, *2 (9)*, 907–914. DOI: https://doi.org/10.1039/b908135f

[10] I. Iliuta, R. Tahoces, G. Patience, *AIChE J.* **2010**, *56 (4)*, 1063–1079. DOI: https://doi.org/10.1002/aic.11967

[11] A. Abad, P. Gayán, L. F. de Diego, F. García-Labiano, J. Adánez, *Chem. Eng. Sci.* **2013**, *87 (87)*, 277–293. DOI: https://doi.org/10.1016/j.ces.2012.10.006

[12] P. Moldenhauer, S. Sundqvist, T. Mattisson, C. Linderholm, *Int. J. Greenhouse Gas Control* **2018**, *71*, 239–252. DOI: https://doi.org/10.1016/j.ijggc.2018.02.021

[13] F. J. Velasco-Sarria, C. R. Forero, E. Arango, *Dyna Energía y sostenibilidad* **2017**, *6 (1)*, 1–20. DOI: https://doi.org/10.6036/ES8139

[14] H. Leion, V. Frick, F. Hildor, *Energies* **2018**, *11 (10)*, 2505. DOI: https://doi.org/10.3390/en11102505

[15] T. Mendiara, L. F. F. de Diego, F. García-Labiano, P. Gayán, A. Abad, J. Adánez, *Fuel* **2014**, *126*, 239–249. DOI: https://doi.org/10.1016/j.fuel.2014.02.061

[16] T. Berdugo Vilches, F. Lind, M. Rydén, H. Thunman, *Appl. Energy* **2017**, *190*, 1174–1183. DOI: https://doi.org/10.1016/j.apenergy.2017.01.032

[17] E. J. Anthony, *Ind. Eng. Chem. Res.* **2008**, *47 (6)*, 1747–1754. DOI: https://doi.org/10.1021/ie071310u

[18] H. Jin, M. Ishida, *Fuel* **2004**, *83 (17–18)*, 2411–2417. DOI: https://doi.org/10.1016/j.fuel.2004.06.033

[19] T. Mattisson, A. Lyngfelt, H. Leion, *Int. J. Greenhouse Gas Control* **2009**, *3 (1)*, 11–19. DOI: https://doi.org/10.1016/j.ijggc.2008.06.002

[20] T. Mendiara, P. Gayán, A. Abad, L. F. De Diego, J. Adánez, *Fuel* **2013**, *106*, 814–826. DOI: https://doi.org/10.1016/j.fuel.2012.11.047

[21] H. Sun, M. Cheng, D. Chen, L. Xu, Z. Li, N. Cai, *Ind. Eng. Chem. Res.* **2015**, *54 (35)*, 8743–8753. DOI: https://doi.org/10.1021/acs.iecr.5b02136

[22] H. Sun, M. Cheng, Z. Li, N. Cai, *Ind. Eng. Chem. Res.* **2016**, *55 (8)*, 2381–2390. DOI: https://doi.org/10.1021/acs.iecr.5b03970

[23] P. Gayán, A. Abad, L. F. de Diego, F. García-Labiano, J. Adánez, *Chem. Eng. J.* **2013**, *233*, 56–69. DOI: https://doi.org/10.1016/j.cej.2013.08.004

[24] H. Thunman, F. Lind, C. Breitholtz, N. Berguerand, M. Seemann, *Fuel* **2013**, *113*, 300–309. DOI: https://doi.org/10.1016/j.fuel.2013.05.073

[25] M. Schmitz, C. Linderholm, *Fuel* **2018**, *231*, 73–84. DOI: https://doi.org/10.1016/j.fuel.2018.05.071

[26] R. Xiao, L. Chen, C. Saha, S. Zhang, S. Bhattacharya, *Int. J. Greenhouse Gas Control* **2012**, *10*, 363–373. DOI: https://doi.org/10.1016/j.ijggc.2012.07.008

[27] C. Linderholm, A. Lyngfelt, A. Cuadrat, E. Jerndal, *Fuel* **2012**, *102*, 808–822. DOI: https://doi.org/10.1016/j.fuel.2012.05.010

[28] S. Sundqvist, M. Arjmand, T. Mattisson, M. Rydén, A. Lyngfelt, *Int. J. Greenhouse Gas Control* **2015**, *43*, 179–188. DOI: https://doi.org/10.1016/j.ijggc.2015.10.027

[29] J. Adánez, P. Gayán, I. Adánez-Rubio, A. Cuadrat, T. Mendiara, A. Abad, F. García-Labiano, L. F. De Diego, *Energy Procedia* **2013**, *37*, 540–549. DOI: https://doi.org/10.1016/j.egypro.2013.05.140

[30] T. Mendiara, L. F. de Diego, F. García-Labiano, P. Gayán, A. Abad, J. Adánez, *Int. J. Greenhouse Gas Control* **2013**, *17*, 170–182. DOI: https://doi.org/10.1016/j.ijggc.2013.04.020

[31] C. Linderholm, M. Schmitz, P. Knutsson, A. Lyngfelt, *Fuel* **2016**, *166*, 533–542. DOI: https://doi.org/10.1016/j.fuel.2015.11.015

[32] R. Pérez-Vega, A. Abad, P. Gayán, F. García-Labiano, M. T. Izquierdo, L. F. de Diego, J. Adánez, *Fuel Process. Technol.* **2020**, *197*, 106184. DOI: https://doi.org/10.1016/j.fuproc.2019.106184

[33] B. Bhui, P. Vairakannu, *J. Environ. Manage.* **2019**, *231*, 1241–1256. DOI: https://doi.org/10.1016/j.jenvman.2018.10.092

[34] J. Fan, H. Hong, L. Zhu, Z. Wang, H. Jin, *Energy Convers. Manage.* **2017**, *135*, 200–211. DOI: https://doi.org/10.1016/j.enconman.2016.12.022

[35] P. Wang, N. Means, B. H. Howard, D. Shekhawat, D. Berry, *Fuel* **2018**, *217*, 642–649. DOI: https://doi.org/10.1016/j.fuel.2017.12.102

[36] W. Bi, T. Chen, R. Zhao, Z. Wang, J. Wu, J. Wu, *RSC Adv.* **2015**, *5 (44)*, 34913–34920. DOI: https://doi.org/10.1039/c5ra02044a

[37] P. Chen, X. Sun, M. Gao, J. Ma, Q. Guo, *Chem. Eng. J.* **2019**, 389–399. DOI: https://doi.org/10.1016/j.cej.2019.02.041

[38] J. Ma, J. Wang, X. Tian, H. Zhao, *Proc. Combust. Inst.* **2019**, *37 (4)*, 4389–4397. DOI: https://doi.org/10.1016/j.proci.2018.07.032

[39] Z. Yaqub, B. Oboirien, *ACS omega* **2020**, *5 (35)*, 22420–22429. DOI: https://doi.org/10.1021/acsomega.0c02880

[40] M. Keller, H. Leion, T. Mattisson, A. Lyngfelt, *Combust. Flame* **2011**, *158 (3)*, 393–400. DOI: https://doi.org/10.1016/j.combustflame.2010.09.009

[41] H. Leion, A. Lyngfelt, M. Johansson, E. Jerndal, T. Mattisson, *Chem. Eng. Res. Des.* **2008**, *86 (9)*, 1017–1026. DOI: https://doi.org/10.1016/j.cherd.2008.03.019

[42] G. L. Schwebel, H. Leion, W. Krumm, *Chem. Eng. Res. Des.* **2012**, *90 (9)*, 1351–1360. DOI: https://doi.org/10.1016/j.cherd.2011.11.017

[43] G. Zhang, O. Ostrovski, *Int. J. Miner. Process.* **2002**, *64 (4)*, 201–218. DOI: https://doi.org/10.1016/S0301-7516(01)00055-2

[44] H. Leion, T. Mattisson, A. Lyngfelt, *Fuel* **2007**, *86 (12–13)*, 1947–1958. DOI: https://doi.org/10.1016/j.fuel.2006.11.037

[45] A. Ramos, E. Monteiro, V. Silva, A. Rouboa, *Renewable Sustainable Energy Rev.* **2018**, *81*, 380–398. DOI: https://doi.org/10.1016/j.rser.2017.07.025

[46] H. Leion, T. Mattisson, A. Lyngfelt, *Int. J. Greenhouse Gas Control* **2008**, *2 (2)*, 180–193. DOI: https://doi.org/10.1016/S1750-5836(07)00117-X

[47] H. Leion, A. Lyngfelt, T. Mattisson, *Chem. Eng. Res. Des.* **2009**, *87 (11)*, 1543–1550. DOI: https://doi.org/10.1016/j.cherd.2009.04.003

[48] J. Ma, X. Tian, C. Wang, X. Chen, H. Zhao, *Int. J. Greenhouse Gas Control* **2018**, *75*, 98–106. DOI: https://doi.org/10.1016/j.ijggc.2018.05.002

[49] H. Xu, J. Ma, H. Zhao, *Chem. Eng. J.* **2018**, *348*, 978–991. DOI: https://doi.org/10.1016/j.cej.2018.05.025

[50] L. Shen, J. Wu, Z. Gao, J. Xiao, *Combust. Flame* **2009**, *156 (7)*, 1377–1385. DOI: https://doi.org/10.1016/j.combustflame.2009.02.005

[51] P. Wang, N. Means, D. Shekhawat, D. Berry, M. Massoudi, *Energies* **2015**, *8 (10)*, 10605–10635. DOI: https://doi.org/10.3390/en81010605

[52] N. Khakpoor, E. Mostafavi, N. Mahinpey, H. De la Hoz Siegler, *Energy* **2019**, *169*, 329–337. DOI: https://doi.org/10.1016/j.energy.2018.12.056

[53] P. Markström, C. Linderholm, A. Lyngfelt, *Int. J. Greenhouse Gas Control* **2013**, *15*, 150–162. DOI: https://doi.org/10.1016/j.ijggc.2013.01.048

[54] J. Adánez, A. Abad, T. Mendiara, P. Gayán, L. F. de Diego, F. García-Labiano, *Prog. Energy Combust. Sci.* **2018**, *65*, 6–66. DOI: https://doi.org/10.1016/j.pecs.2017.07.005

[55] H. Gu, L. Shen, Z. Zhong, X. Niu, H. Ge, Y. Zhou, S. Xiao, *Ind. Eng. Chem. Res.* **2014**, *53 (33)*, 13006–13015. DOI: https://doi.org/10.1021/ie501328h

[56] J. Yan, L. Shen, Z. Ou, J. Wu, S. Jiang, H. Gu, *Energy* **2019**, *167*, 168–180. DOI: https://doi.org/10.1016/j.energy.2018.09.075

[57] A. Abad, T. Mendiara, L. F. de Diego, F. García-Labiano, P. Gayán, J. Adánez, *Fuel Process. Technol.* **2018**, *179*, 444–454. DOI: https://doi.org/10.1016/j.fuproc.2018.07.031

[58] A. Abad, P. Gayán, R. Pérez-Vega, F. García-Labiano, L. F. de Diego, T. Mendiara, M. T. Izquierdo, J. Adánez, *Fuel* **2020**, *271*, 117514. DOI: https://doi.org/10.1016/j.fuel.2020.117514

